Chapter 1

Low Dimensional Magnetism

Nowadays, various compounds have been synthesized which serve as model systems for the investigation of quantum spin systems with a one-dimensional arrangement of spins. By adding neighboring chains of spins, ladder systems can evolve into a model for two-dimensional spin configurations.

Experimental studies on spin-chain systems with antiferromagnetic order have clearly established the difference between half-integer and integer spin-chain systems with respect to the appearance of a gap in the excitation spectrum of the latter (Haldane's conjecture). The presented investigations show neutron scattering studies on spin-ladder and spin-chain compounds in order to reveal the magnetic structure and excitation spectra in the presence of a magnetic field.

The field-dependent data in $Cs_3Cr_2Br_9$ show the persistence of an energy gap in the field induced magnetic phase in the spin-excitation spectra of this system with weakly coupled dimers of $S = 3/2$-spins. This observation excludes the possible existence of a Bose-Einstein condensation with gap-less excitations as might have occurred in this system. For the investigated NTENP compound belonging to the family of spin-1 chains, the existence of alternating bonds along the spin chain has an influence on the dispersion of the magnetic excitations and on the field dependence of the excitation energies. Polarized neutron scattering studies in the compound $Sr_{14}Cu_{24}O_{41}$ containing both spin ladders and chains reveal a strong anisotropy in the magnetic structure factors.

1.1 Ordering and excitations in the field induced magnetic phase of $Cs_3Cr_2Br_9$.

B. Grenier and L.P. Regnault
Collaborations : Y. Inagaki, T. Asano, and Y. Ajiro (Japan), A. Wildes and T. Ziman (ILL, Grenoble), E. Lhotel, C. Paulsen, and J.P. Boucher (CNRS, Grenoble)

$Cs_3Cr_2Br_9$ (CCB) is a quantum spin system consisting of weakly coupled dimers of Cr^{3+} ions with spin $s = 3/2$. This compound shows a gap E_G in its energy spectrum, between the $S = 0$ singlet ground state and the $S = 1$ triplet state. When applying a magnetic field H, such a system shows peculiar physical properties. When the gap closes at a critical field H_{c1} ($g\mu_B H_{c1} \sim E_G$), a three-dimensional magnetic ordering develops, due to the small inter-dimer couplings. In this field-induced magnetic ordering (FIMO), the antiferromagnetically (AF) ordered magnetic moments lie in the plane perpendicular to the applied field (*transverse AF ordering*), while a small ferromagnetic component arises parallel to H (z-axis). A Bose-Einstein condensation of gapless excitations might then occur, at the FIMO transition [1]. Indeed, a gapless Goldstone mode was claimed to be observed recently in the $s = 1/2$ dimer compound $TlCuCl_3$ [2] at the critical field.

$Cs_3Cr_2Br_9$ has been widely investigated at low field ($H < H_{c1}$) by Leuenberger *et al.* [3], yielding in particular the following parameters: $J = 1.03$ meV for the intra-dimer coupling, $J_p = 0.054$ and $J_c = 0.039$ meV for the in-plane and out-of-plane inter-dimer couplings, respectively (shown in Fig. 1.1). CCB differs from $TlCuCl_3$ both by the larger spin values involved in the dimer (lying along the $c-$axis) and by the hexagonal crystallographic arrangement (in the (a, b) plane) of the dimers. These two peculiarities are expected to favor local anisotropies in the magnetic couplings and frustration, respectively, and should have some important consequences on the properties of the FIMO phase. It is thus of great interest to study both the magnetic ordering and the spin excitations in the FIMO phase of CCB.

Neutron scattering experiments were realized on a large single crystal ($\sim$ 350 mm^3) mounted in a 6 T vertical cryomagnet equipped with a dilution insert ($T \sim 50-100$ mK), and the $\mathbf{a} - \mathbf{b}$ direction of the crystal was set vertically (parallel to $\mathbf{H}$). The elastic investigation was performed on the lifting arm two-axis diffractometer CRG-CEA D23 while the inelastic one was performed on the triple-axis spectrometer CRG-CEA/FZ IN12, both installed at the Institut Laue Langevin (ILL).

Magnetic structure

In the diffraction experiment on CCB, 113 nuclear reflections, reducing to 68 independent ones, were collected. The structural refinement (12 parameters) was achieved with type II Becker-Coppens Gaussian extinction correction and isotropic thermal factors. A weighted $R-$factor of 1.7 % was obtained on the nuclear structure factors. 123 magnetic reflections were then collected at $H = 6$ T in the three magnetic domains. Indeed, for symmetry reasons, the three following commensurate propagation vectors were found: $\mathbf{k}_1 = (1/4, 1/4, 0)$, $\mathbf{k}_2 = (-1/2, 1/4, 0)$, and $\mathbf{k}_3 = (1/4, -1/2, 0)$. The magnetic refinement, using an isotropic Cr^{3+} magnetic form factor, leads to a weighted $R-$factor of 4.2 % on the magnetic structure factors and gives the following information (see Fig. 1.1): **a-** the populations of the three domains are about the same (34.8 $\pm$ 0.6, 33.0 $\pm$ 0.4, and 32.3 $\pm$ 0.4 %); **b-** the magnetic structure is colinear with the moments pointing along the **c** ($\equiv x$) axis, thus perpendicular to H as expected for a FIMO phase; **c-** the spin arrangement within one unit cell is shown by the atoms labelled 1, 2, 3, 4; **d-** this motif propagates with the sequence $++--$, assuming the moment amplitude to be constant, along the direction of **k** ((110) for the first domain); **e-** the AF transverse moment amplitude derived from the refinement is $M_{AF} = 1.60(1)\ \mu_B$ per Cr^{3+} ion at $H = 6$ T. In addition to the transverse magnetization, the parallel one was determined from the ferromagnetic contribution appearing on top of the weak nuclear Bragg peak $(1, 1, 4)$: $M_{\parallel} = 0.37(3)\ \mu_B$ at 6 T.

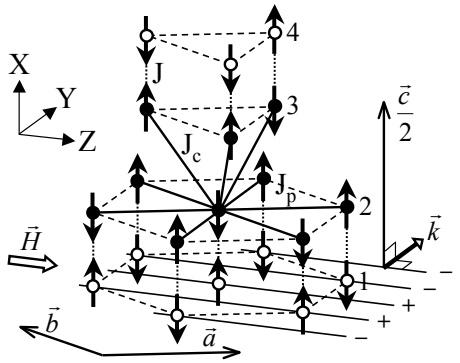

Figure 1.1: Transverse $++--$ AF spin ordering of the Cr^{3+} ions at 6 T for $\mathbf{H} \parallel \mathbf{a}-\mathbf{b}$. This picture corresponds to the first magnetic domain of the FIMO phase.

The field dependence of the propagation wave-vector component k and that of the transverse magnetic moment M_{AF} were studied between 0 and 6 T (see

[1] I. Affleck, Phys. Rev. B **43**, 3215 (1991)
[2] Ch. Rüegg *et. al.*, Nature **423**, 62 (2003)
[3] B. Leuenberger *et. al.*, Phys. Rev. B **30**, 6300 (1984)

open and closed circles in Fig. 1.2). These data were obtained from scans performed in the (110) direction across the strongest magnetic peak $(1-k,\ 1-k,\ 2)$ with $k \sim 0.25$, for increasing and decreasing magnetic field, respectively. Each scan could be well fitted by a Gaussian function, whose position and integrated intensity gave accurate values for k and M_{AF}^2 respectively. When increasing (decreasing) H, the $(1-k,\ 1-k,\ 2)$ peak could be detected from (down to) $H \sim 1.5$ T, giving a critical field H_{c1} slighly lower than this value. Interestingly, incommensurabilities and large hysteresis effects can be observed in Fig. 1.2 (a), suggesting first order transitions: For increasing field, the FIMO becomes commensurate only from $H \sim 5$ T, while for decreasing field, the transverse commensurate $++--$ ordering remains locked down to $H \sim 3$ T and then becomes incommensurate (k shifts progressively from $k = 0.25$ to 0.29 r.l.u. at 1.5 T). Note that a small jump is also observed in $M_{AF}(H)$, for decreasing H, at the same field (see Fig. 1.2). The *parallel* magnetization $M_{//}(H)$ (Fig. 1.2) was obtained from SQUID measurements performed at $T \sim 100$ mK in the full field range (solid triangles). These data are in good agreement with the value of $M_{//}$ estimated at 6 T from neutron scattering (open triangle).

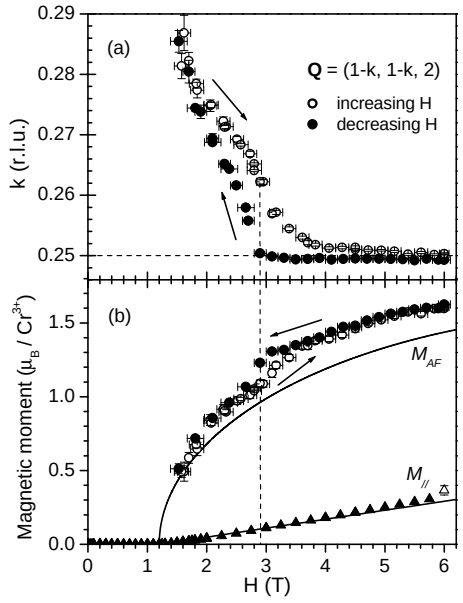

Figure 1.2: (a) Field-dependence of the propagation wave-vector component k and (b) that of the transverse (M_{AF}) and parallel ($M_{//}$) magnetizations. The solid lines are theoretical predictions obtained for the commensurate $++--$ magnetic order in Ref. [92].

Spin dynamics

We have studied the dispersion curve along $a^* + b^*$ as a function of the applied field, between 0 and 6 T, and the position of the energy gap was found to be field-independent: $\mathbf{Q^0} = (0.27, 0.27, 2)$, though the wave vector component k of the magnetic structure varies between 0.25 and 0.29 r.l.u. above H_{c1}. We focus here on the field dependence of the energy gap for the three branches of the $S = 1$ triplet state (see Fig. 1.3), obtained from energy scans performed at (0.27, 0.27, 2). The inset of Fig. 1.3 shows such a scan recorded at $H = 0$: A splitting - *not detected previously by Leuenberger et al.* - is clearly observed. It reveals the presence of a single-ion anisotropy at each Cr^{3+} site which can be described by a term $D(s_i^x)^2$. The observed splitting can be accounted for by redefining for each branch two distinct effective intra-dimer couplings $J^+ = J + 0.8D$ and $J^- = J - 1.6D$ with $D \sim -0.01$ meV. With this value, the Zeeman splitting below H_{c1} (solid lines in fig. 1.3) agrees also very well with the data. From the lowest energy branch, the critical field is expected at $H_{c1} \sim 1.5$ T, consistently with the elastic study. For $H > H_{c1}$, three distinct branches are still observed. The two upper branches agree roughly with "Zeeman" behaviors, $\sim g\mu_B H$ and $\sim 2g\mu_B H$ (dotted lines). Unexpectedly, the gap of the lowest energy branch ($\mathcal{E}_g$) never closes in the full field range of the FIMO phase, even at $H = H_{c1}$. This new result shows that *there is no gapless Goldstone mode in the FIMO phase of* $Cs_3Cr_2Br_9$. It could be well explained by the presence of the single-ion anisotropy acting in the *transverse xy* plane ($x = \mathbf{c}$, $y = \mathbf{a} + \mathbf{b}$). An analysis in terms of projected pseudo-spins, detailed in Ref. [92], allowed to reproduce $\mathcal{E}_g(H)$ (dashed line in Fig. 1.3).

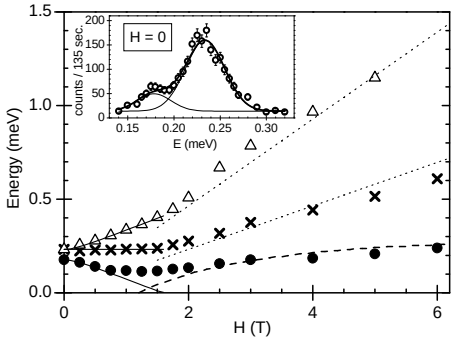

Figure 1.3: Field dependence of the energy gaps. Inset: $H = 0$ energy scan performed at (0.27, 0.27, 2).

Conclusion

The elastic study of $Cs_3Cr_2Br_9$ has revealed new properties for a FIMO phase: incommensurability and hysteresis, which can be accounted for by the frustrating (ferromagnetic) couplings present in the $++--$ magnetic order, as shown in Fig. 1.1. The inelastic study has also established new results: the existence of a small single-ion anisotropy and the presence at $H \geq H_{c1}$ of a gap in the lowest excitation branch. This anisotropy is of crucial importance since it explains the relatively large energy gap observed in the FIMO phase of $Cs_3Cr_2Br_9$.

1.2 Spin dynamics in the S=1 bond-alternating antiferromagnetic chain compound NTENP.

L.P. Regnault
Collaborations : M. Hagiwara (RIKEN, Japan), K. Kakurai (JAERI, Japan), and A. Stunault (ILL, Grenoble)

Since the Haldane's prediction enounced in 1983, integer-spin Heisenberg antiferromagnetic chains are believed to behave quite differently from half-odd integer spin chains [4]. In particular, the ground state of the spin-1 chain should be a non-magnetic singlet ground state, well separated from the first triplet excited states by a large gap (Haldane's conjecture). This non-intuitive result has been verified on the compound $Ni(en)_2NO_2ClO_4$ (alias NENP), a prototype of the S=1 Heisenberg chain with single-ion anisotropy [5]. Recently, it has been suggested [6] that the presence of a sizable alternating exchange term could modify severely the nature of the ground state.

The spin system that we will consider in this contribution is described by the following Hamiltonian:

$$H = J_{av} \sum_i [1 - (-1)^i \delta] \mathbf{S}_i \cdot \mathbf{S}_{i+1} + D \sum_i (S_i^z)^2 \quad (1.1)$$

where J_{av} is the average coupling constant between two adjacent spins, δ represents the asymmetry of couplings (alternating exchange) and D is the single ion anisotropy. In what follows, it will be useful to consider the alternation parameter α, related to δ by the relation: $\alpha = \frac{1-\delta}{1+\delta}$. For $D \approx 0$ and varying α, Yamamoto predicted gap-values of $0.41 J_{av}$ for $\alpha = 1$ (pure Haldane system) and of $2J_{av}$ for $\alpha = 0$ (isolated-dimer system), with a vanishing gap in between for $\alpha = 0.6$. Very recently, Narumi et *al* [7] have investigated the magnetic properties of the nickel-based compound Ni(333-tet)μ-NO_2ClO_4 [333-tet=N,N′-bis(3-aminopropyl)propane-1,3-diamine] (abbreviated as NTENP), which indicated that this material was a good realization of a spin chain system described by equation 1.1, with parameters $J_{av} \approx 39$ K (≈ 3.4 meV), $\alpha \approx 0.45$ and a strong ratio $D/J \approx 0.25$. In order to investigate more precisely the ground and excited-state properties, we have undertaken comprehensive inelastic neutron scattering experiments on large-size protonated and fully-deuterated single-crystals.

NTENP crystallizes in the triclinic space group $P\bar{1}$ [8], with cell parameters at room temperature $a = 10.75$ Å, $b = 9.41$ Å, $c = 8.79$ Å, $\alpha = 95.52°$, $\beta = 108.98°$ and $\gamma = 106.83°$. The Ni chains run along the a axis. The inelastic neutron scattering measurements have been performed on the three-axis spectrometers IN12, IN14 and IN22 installed on beams at the ILL high-flux reactor.

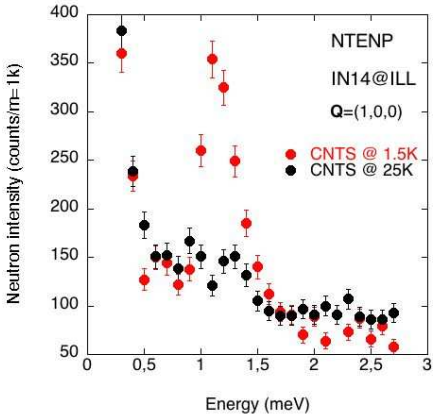

Figure 1.4: Constant-Q scan at $\mathbf{Q} = (1, 0, 0)$ for two temperatures T=1.5 and 25 K, showing the existence of a well-defined gap of magnetic origin at energy 1.2 meV.

Figure 1.4 shows an energy scan performed at the scattering vector $\mathbf{Q} = (1, 0, 0)$ at 1.5 and 25 K.

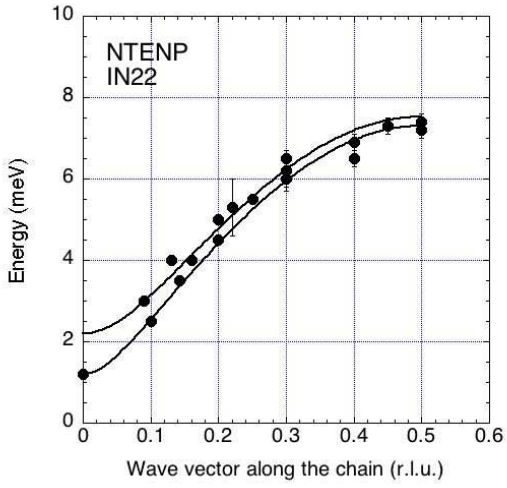

Figure 1.5: Dispersion of the two magnetic excitations along the [1 0 0] chain direction.

Quite unambiguously, the low-temperature scan displays a sharp peak centered at the energy $\Delta_{bc} \approx 1.2$ meV, characteristic of the opening of a gap in the magnetic excitation spectrum. The 1.2-meV mode vanishes almost completely at 25 K, this among other proving its magnetic origin. Constant-energy and constant-Q scans performed on IN14 and IN22 along the [1 0 0] chain direction over the entire Brillouin zone showed that the mode is dispersive with a maximum energy $\omega_{max} \approx 7.5$

[4] F.D.M. Haldane, Phys. Rev. Lett. **50**, 1153 (1983)
[5] L.P. Regnault et *al.*, Phys. Rev. B **50**, 9174 (1994)
[6] S. Yamamoto, Phys. Rev. B **52**, 10170 (1995)
[7] Y. Narumi et *al.*, Phys. Rev. Lett. **86**, 323 (2001)
[8] A. Escuer et *al*, J. Chem. Soc.Dalton Trans, 531 (1997)

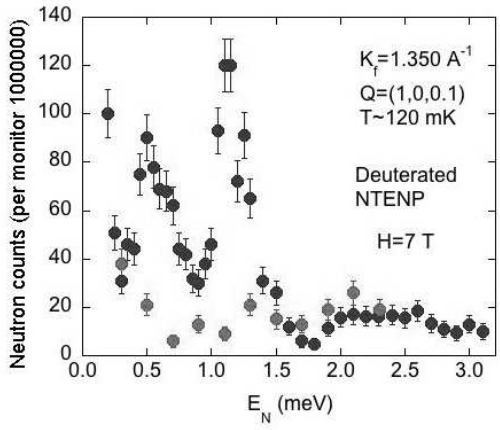

Figure 1.6: Constant-Q scan at 7 Tesla showing the splitting of the 1-meV mode under field.

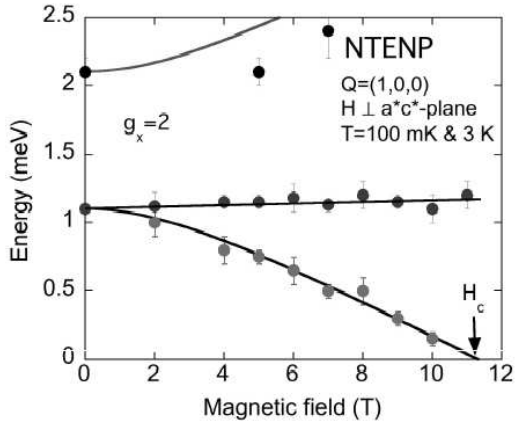

Figure 1.7: Field dependence of the two low energy gaps.

meV. The full dispersion curve is given in Fig.1.5. In this figure, the solid line is a fit to the theoretical sine-wave dispersion relation:

$$\hbar\omega(Q_a) \approx \sqrt{(\Delta^2 + \omega_{max}^2 \sin^2(\pi(1-Q_a))} \qquad (1.2)$$

with parameters $\Delta \approx 1.2$ meV and $\omega_{max} \approx 7.5$ meV. Careful measurements performed on IN22 at the scattering vector $\mathbf{Q} = (-1, 0, 3.2)$ have allowed to further determine the in-chain gap energy $\Delta_a \approx 2$ meV. This observed splitting of the spin excitation reflects the strong planar (D positive) anisotropy anticipated from the susceptibility and magnetization data.

A comprehensive investigation on IN12 under magnetic fields up to 12 Tesla has revealed the triplet nature of magnetic excitations at $q \approx \pi$ and allowed us to follow the field dependences of gaps on both sides of the critical field $H_c^b \approx 11.4T$. Fig.1.6 shows a typical constant-Q scan performed at 7 T and 120 mK, which unambiguously demonstrates the two-fold degeneracy of the 1.2-meV mode. The whole set of so far experimentally obtained energy gaps and the comparison with the field-theory results is depicted in Fig.1.7. From the theoretical point of view, the elementary excitation spectrum of the S=1 antiferromagnetic Heisenberg chain with bond alternation was investigated long time ago by Yamamoto [9]. For $\alpha \approx 0.40 - 0.45$ (i.e. $\delta \approx 0.38 - 0.43$), the calculation gives $\Delta \approx 0.3 J_{av}$ and $\omega_{max} \approx 2.2 J_{av}$. A rather good agreement between theory and experiment is obtained by taking an average coupling constant $J_{av} \approx 3.4$ meV and an anisotropy constant $D \approx 0.8$ meV, values found in good agreement with those previously derived from suceptibility and magnetization measurements. Surprisingly and without explanation so far, the gap average $\Delta_0 = (2\Delta_{bc} + \Delta_a)/3 \approx 1.43$ meV (expected to reflect the gap value in the absence of anisotropy), indeed coincides precisely with the Haldane-gap ($\alpha = 1$) value, $\Delta_0/J_{av} \approx 0.41$.

[9] S. Yamamoto, Phys. Rev. B **51**, 16128 (1995)

1.3 Pressure effect in NaV_2O_5

B. Salce and J.Y. Henry

Low-dimensional magnetic compounds are extensively studied in order to understand the role played by the magnetic interactions in phase transitions. The germanate $CuGeO_3$ is the first inorganic material which exhibits, below the temperature $T_{SP} = 14.3$ K, a structural distortion driven by antiferromagnetic interactions in the one-dimensional spin-1/2 Heisenberg chains, the so-called "spin-Peierls" (SP) transition. With a layered structure, NaV_2O_5 belongs to low-dimensional quantum spin systems and was at first believed to undergo a conventional SP transition below $T = 34$ K. A more accurate description of this transition is now well established: extensive work (particularly the neutron experiments performed at SPSMS) has demonstrated that a charge-ordering (CO) transition occurs from one type of vanadium site, $V^{4.5+}$, at room temperature, to two different states of oxidation for the vanadium atoms (V^{4+} and V^{5+}) below the charge ordering temperature T_{CO}. Hydrostatic pressure P is a powerful parameter for the understanding of such compounds, as it allows to influence the "spin-spin" and the "spin-lattice" couplings via the change in interatomic distances. Recently, we investigated the behaviour of $CuGeO_3$ under pressure up to 10 GPa [69]. Specific heat C(T,P) experiments were carried out by using an alternative calorimetry (ac) method in a diamond anvil cell. Using "in-situ" pressure variation, we were able to get pressure steps smaller than .3 GPa with argon as pressure transmitting medium and ruby fluorescence as pressure gauge. The obtained evolution of T_{SP} with the pressure is shown in Fig. 1.8. T_{SP} increases monotonously in the whole pressure range with two different linear regimes below and above $P_C \simeq 2$ GPa. A possible explanation to interpret this behaviour could be the occurrence of a new structural transition at P_C. The C(T,P) measurements were carried out on NaV_2O_5 single crystals grown at SPSMS. The C(T, P=0) experiment was performed by means of a classical adiabatic method showing, around $T_{CO} = 34$ K, a nice signal which favourably compared to the ones obtained by other groups. The experimental set-up used for experiments under pressure was identical to the one previously described. At low pressure, the signature of the transition was recorded both in modulus and phase components, but only the phase signal could be detected above 1.5 GPa. The data collected up to 4 GPa from two different samples are plotted in figure 1 in order to be directly compared with the $CuGeO_3$ results.

Contrary to the case for $CuGeO_3$, T_{CO} decreases in the whole pressure range. At low pressures, the rate of -12 K/GPa agrees with results from [10]. However, as a new fact, around $P_C = 2$ GPa, a change of slope is observed similar to the one in $CuGeO_3$. The work by Ohwada et al. has shown that NaV_2O_5 undergoes, from

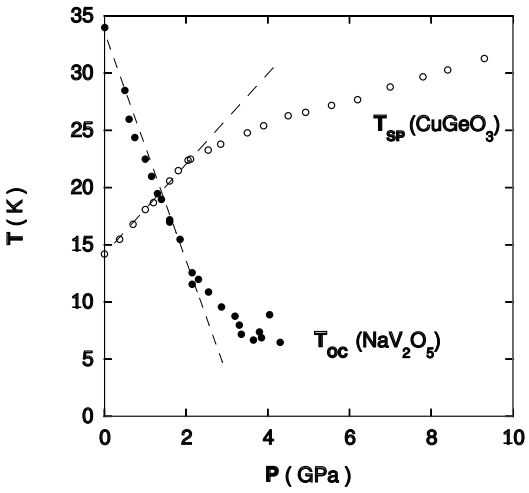

Figure 1.8: Evolution of the transition temperatures with the pressure in $CuGeO_3$ and NaV_2O_5 for respectively the spin-Peierls and charge-ordering transitions.

.5 to 1.2 GPa, many structural transitions which have been explained in the framework of a simple model with competitive inter-layer interactions, but in this pressure range the T_{CO} variation remains constant. This observation could be an argument to rule out the idea that the existence of P_C is connected with a structural distortion. In this case, the role of frustration could be invoked to understand the behaviour of T_{CO} in NaV_2O_5 under high pressures.

To summarize, the opposite pressure variation measured on T_{SP} and T_{CO} stress the major difference between the two compounds, but it is puzzling to observe that a "critical" pressure P_C exists in both systems. Further investigations will be undertaken in order to understand these features.

[10] K. Ohwada et al., Phys. Rev. Letters, **87**, 86402 (2001)

1.4 Polarised neutron investigation of the magnetic and lattice excitations in the chain-ladder system $Sr_{14}Cu_{24}O_{41}$.

C. Boullier and L.P. Regnault
Collaborations : J.E. Lorenzo(CNRS, Grenoble), G. Dhalenne(Université de Paris-Sud, Orsay) and A. Revcolevschi(Université de Paris-Sud, Orsay)

For the understanding of high-T_c superconductivity in the cuprates physicists are lead to study materials with related crystallographic structures showing similar electronic processes. Among those materials, the spin-ladder compound $Sr_{14}Cu_{24}O_{41}$ (SCO) is a good candidate to investigate. Its crystallographic structure is a misfit stacking of layers of two distinct quantum-spin systems: linear edge-sharing CuO_2 chains and 2-leg Cu_2O_3 spin-ladders (see Fig. 1.9 - **c** is along the chains, **a** is in the plane and **b** is out of the plane -) . The pure compound naturally contains hole carriers which are mainly located in the chains and by substitution of Ca for Sr, some holes are transferred from the chains to the ladders and an insulator-to-metal transition appears. Furthermore, by applying a high pressure(3 GPa) on a highly Ca-doped compound, superconductivity is observed with a critical temperature of the order of 10 K. Thus, this hole-transfer mechanism leading to superconductivity is very similar to the one observed in the high-T_c superconductors $YBa_2Cu_3O_{6+\delta}$ and the characterisation of magnetic excitations in this spin-ladder compound may provide a better understanding of the role of magnetism in the pairing mechanism.

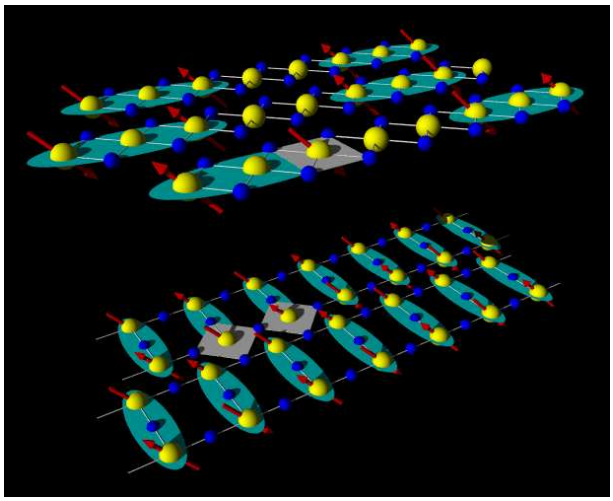

Figure 1.9: Cristallographic structure and magnetic dimers in the chain and ladder sub-systems of $Sr_{14}Cu_{24}O_{41}$.

In order to better understand the nature of excitation spectra in $Sr_{14}Cu_{24}O_{41}$, we recently performed accurate polarimetric inelastic-neutron-scattering studies of the chain and ladder excitations in this compound. By measuring the spin-flip and non spin-flip contributions for the incident polarisation applied parallel and perpendicular to the scattering vector Q we have been able to separate the nuclear from other magnetic components. Quite unexpectedly, our results reveal the existence of a strong anisotropy of the magnetic inelastic structure factors, which could be the signature of orbital currents predicted theoretically.

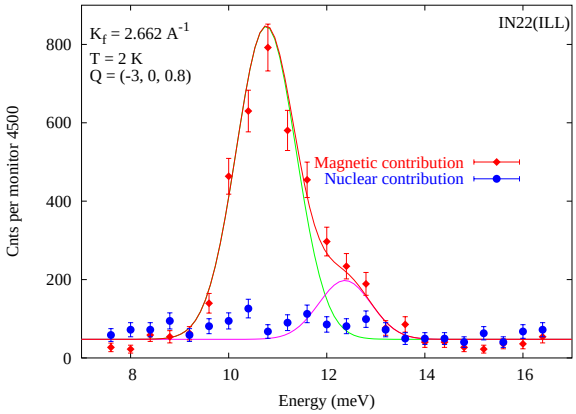

Figure 1.10: Inelastic scan with polarized neutrons, showing two purely magnetic modes in the chain sub-system .

In the two sub-systems, the existence of magnetic dimers leads to the opening of magnetic gaps in the inelastic spectra. From unpolarized inelastic neutron scattering (INS) measurements, it has been shown that the magnetic excitation spectrum in the chain subsystem is made of two branches weakly dispersive in the (**a**, **c**) plane, both associated with singlet-triplet transitions originating from the existence of weakly interacting dimers ↑-hole-↓, with transition energies ≈ 11 meV [11]. The magnetic excitation spectrum of the ladder subsystem exhibits a strongly dispersive mode above a gap energy $\Delta_L \approx$ 32-33 meV at the position of the AF wave vector[12].

In order to probe the exact nature of elementary excitations in the chain and ladder sub-systems of SCO (in particular the possible existence of hybride modes), we have recently performed longitudinal polarisation analysis experiments on the CRG three-axis spectrometer IN22. Figure 1.10 shows a typical constant-Q scan performed at the scattering vector **Q** = (-3, 0, 0.8), characteristic of the chain sub-system, with the incident polarisation kept parallel to **Q** during the scan. Within this configuration, one is able to separate unambiguously the magnetic (all spin-flip) and structural (all non spin-flip) contributions. At the accuracy of the measurements, no structural components could be detected, thus confirming the purely magnetic nature of both modes at 11

[11] L.P. Regnault *et al.*, *Phys. Rev. B* **59** (1999) 1055
[12] R. S. Eccleston *et al.*, *Phys. Rev. B* **53** (1996) 14721

and 12.2 meV. Interestingly, the peaks are resolution-limited, implying a very weak intrinsic splitting of the triplet modes. Figure 1.11 shows a similar constant-Q scan performed at the scattering vector $\mathbf{Q}$ = (-4.5, 0, 0.5) characteristic of the ladder sub-system, which again confirms both the purely magnetic nature and the degeneracy of the triplet gap at Δ_L.

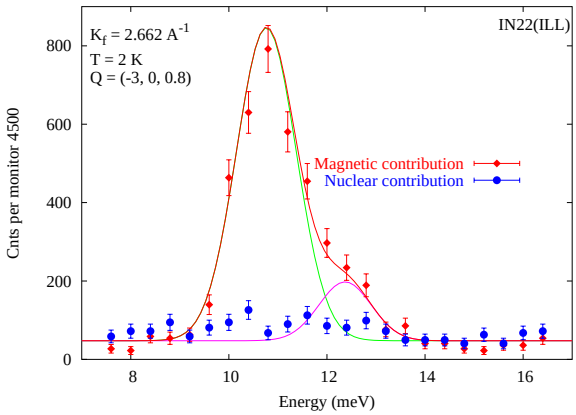

Figure 1.11: Inelastic scan with polarized neutrons, showing two purely magnetic modes in the ladder sub-system .

From the structural point of view, the octahedral environment of a single copper ion (see pink squares in Fig. 1.9) is similar in the ladder and in the chain sub-system, so the anisotropy of the Landé g-factor is expected to be similar in both systems. It is not possible to perform measurements of the g-tensor in the ladder sub-system due to the high value of the magnetic gap. However, in the chain sub-system, applying a strong magnetic field perpendicular to the (**a**, **c**) plane, we were able to lift the degeneracy of the triplet state and to determine the Landé g-factor. Due to crossing of the dispersion curves of magnetic excitations in the chain sub-system, the two triplet states are superimposed at $\mathbf{Q}$ = (2.5, 0, 0.25) and we can observe from the scan depicted in Fig. 1.12 that the triplet states are well-defined and resolution-limited in zero field. The inelastic scan at $\mathbf{Q}$ = (2.5, 0, 0.25) under a strong magnetic field of 11.5 Tesla is also shown in the same figure. We clearly observe the splitting of the triplet state into three modes with a splitting $g_b\mu_B H \approx 1.5$ meV. From our measurements, we determine that the g-tensor component along the direction perpendicular to the plane of chains is $g_b = 2.31 \pm 0.06$. This value is very close to the value 2.28±0.03 found recently by ESR[13] and confirms the rather strong anisotropy previously found by magnetic susceptibility measurements on single crystals[14], which can be seen as a signature of strong spin-orbit couplings. However, such an anisotropy is in contradiction with the absence of splitting in the zero field data.

In order to understand this paradoxical situation, we have used the longitudinal polarisation analysis to determine separately the in-plane $S_{\parallel}(Q, \omega)$ and the out-of-plane $S_{\perp}(Q, \omega)$ dynamical structure factors, by measuring the polarization dependence of the scattering cross-sections with the incident polarization applied successively along and perpendicular to the scattering vector $\mathbf{Q}$ in the CuO_2 planes, and perpendicular to these planes. Similar measurements have been performed on the ladder contribution. Quite surprisingly, we observe in both cases a strong anisotropy $\frac{S_{\perp}(Q,\omega)}{S_{\parallel}(Q,\omega)} = 1.4 \pm 0.15$, which means that the two-point correlation functions are much better established for the components perpendicular to the CuO_2 or Cu_2O_3 planes. For the chain sub-system, this result is consistent both with the susceptibility measurements[15] (for which χ_b is 20-30% larger than $\chi_a \approx \chi_c$ below 350 K) and our measurements under field. Indeed at 11.5 T, the integrated intensity of the centred mode (Fig. 1.12) is 1.4 times the sum of the integrated intensities of the side modes, confirming the anisotropy of the magnetic signal.

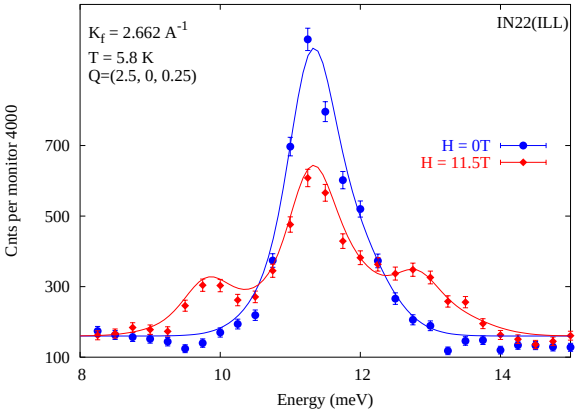

Figure 1.12: Inelastic scan of the magnetic modes in the chain sub-system with H=0 and 11.5 T.

To conclude, the strong anisotropy observed in the dynamical correlation functions together with the absence of a gap splitting in zero-field, lead us to believe that in SCO the Hamiltonian should not be a simple Heisenberg one, but should contain more complicated terms. Indeed, this paradoxical situation could very likely be understood by taking into account the orbital degrees of freedom and the spin-orbit couplings, expected to be strong in $Sr_{14}Cu_{14}O_{41}$.

[13] V. Kataev *et al.*, *Phys. Rev. B* **64** (2001) 10422
[14] M. Matsuda *et al.*, *Phys. Rev. B* **53** (1996) 12201
[15] M. Matsuda *et al.*, *Phys. Rev. B* **53** (1996) 12201

1.5 Quasi-1D spin chains

S. A. Blundell
Collaborations : M. D. Núñez-Regueiro (CNRS Grenoble)

There is currently great interest in the physics of quantum antiferromagnetic (AF) spin systems. More than twenty years ago, Shastry and Sutherland[16] introduced a new class of quantum topological excitation, in which isolated defects separate the system into domains of differing translational symmetry. Since their proposal, the search for both theoretical models and real physical systems showing this behavior has continued. The typical example is the zigzag spin ladder shown in Fig. 1.13(a). Another example, which we shall consider here, is the sawtooth or Δ chain shown in Fig. 1.13(b), a frustrated system consisting of $s = 1/2$ spins coupled antiferromagnetically in the topology of a series of triangles.

We have analyzed [21] [22] [305] the sawtooth lattice in the asymmetric case of unequal antiferromagnetic couplings $J_{\rm bv} \neq J_{\rm bb}$, where $J_{\rm bv}$ is the coupling between a spin on the base of a triangle and a neighboring one on the vertex, and $J_{\rm bb}$ that between two neighboring spins on the base of a triangle. When all couplings are equal ($J_{\rm bv} = J_{\rm bb}$), the ground state is known to be two-fold degenerate and fully *dimerized*, that is, consisting entirely of spin-singlet states between a spin on the base and the neighboring spin on the vertex either to the right (R-dimerization) or to the left (L-dimerization), as shown in Fig. 1.13(c).

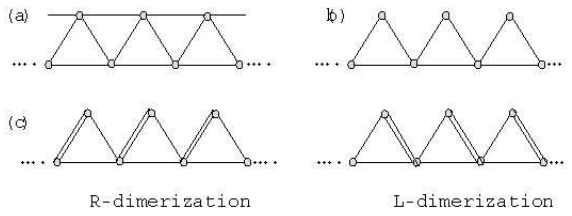

Figure 1.13: Quasi-1D spin chains: (a) the zigzag ladder, (b) the sawtooth or Δ chain, (c) the two degenerate ground states of the Δ chain when all interactions are equal. Double lines indicate the formation of a spin singlet state (or *dimer*).

Despite the great amount of theoretical work that has been performed on these quasi-1D spin chains, there is a lack of clear physical realizations of any of the various models discussed. However, new results have recently become available, following the synthesis[17] of $YCuO_{2.5}$, which from structure measurements appears to be a nice realization of the sawtooth lattice, most likely with $J_{\rm bb} \ll J_{\rm bv}$.

We are unable to solve analytically and exactly for the wave function and dispersion for arbitrary $J_{\rm bb}/J_{\rm bv}$, but many of the important features of the spectrum can be obtained with high numerical precision by a careful exact diagonalization and extrapolation procedure.

[16] B. S. Shastry and B. Sutherland, Phys. Rev. Lett **47**, 964 (1981).
[17] O. Garlea, Thesis Grenoble University (2001).

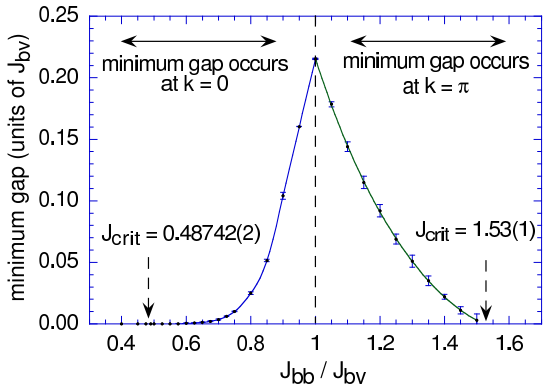

Figure 1.14: Gap to the lowest $S_{\rm tot} = 1$ excited states of the sawtooth lattice, after extrapolation to $N \to \infty$.

We extract the eigenvalues and eigenvectors of the spin Hamiltonian essentially exactly for finite-sized systems with up to 12 triangles (24 spin sites), using iterative methods such as the Lanczos or Davidson methods, and then extrapolate the results to the infinite-size limit.

Figure 1.14 summarizes the behavior of the excitation gap. We find the lowest-lying excitations to have total spin quantum numbers $S_{\rm tot} = 0$ and $S_{\rm tot} = 1$, which are degenerate within numerical error, thus giving a four-fold degeneracy overall. The gap is greatest when the interactions are equal ($J_{\rm bb} = J_{\rm bv}$), but decreases as $J_{\rm bb}/J_{\rm bv}$ moves away from unity; at the same time, the spectrum, which is dispersionless for $J_{\rm bb} = J_{\rm bv}$, acquires increasing dispersion. The gap finally closes at wavevector $k = 0$ for $J_{\rm bb}/J_{\rm bv} < 1$ and at $k = \pi$ for $J_{\rm bb}/J_{\rm bv} > 1$. In this way, the gapped symmetric Δ-chain ($J_{\rm bb} = J_{\rm bv}$) goes over smoothly into the gapless Heisenberg chain ($J_{\rm bb} = 0$ or $J_{\rm bv} = 0$). We have been able to extract the critical couplings for gap closure to high numerical accuracy.

To get some insight into the change of character of the ground state $|0\rangle$ as a function of $J_{\rm bb}/J_{\rm bv}$, we have also considered the ground-state *dimerization fraction* $D_{\rm frac}$, defined as $D_{\rm frac} = |\langle 0|R\rangle|^2 + |\langle 0|L\rangle|^2$, where $|R\rangle$ and $|L\rangle$ are the pure dimer states [Fig. 1.13(c)]. The dimerization fraction drops from its value of unity at $J_{\rm bb} = J_{\rm bv}$ (perfect dimerization) as $J_{\rm bb}/J_{\rm bv}$ decreases, becoming zero within numerical error ($D_{\rm frac} \lesssim 0.02$) when $J_{\rm bb}/J_{\rm bv}$ is less than the critical value for gap closure $(J_{\rm bb}/J_{\rm bv})_{\rm crit} \approx 0.49$ (see Fig. 1.14). This shows that the gap reduction is related to increasing quantum fluctuations of the dimer state.

We hope that this first complete study will assist the interpretation of the experimental results on these zigzag chains.

1.6 Magnetic quantum oscillations in quasi two-dimensional metals.

T. Champel and V.P. Mineev

The quantitative theory of the magnetic quantum oscillations in metals was proposed in 1955 by Lifshitz and Kosevich. It has been verified by many experiments and has been widely used to determine the Fermi surface of metals. The Lifshits-Kosevich theory applies to metals with a three-dimensional (3D) gas of electrons. Recently, there has been a renewed interest in the study of compounds with strongly anisotropic electronic properties in high magnetic fields. For example, in semiconductor heterostructures a 2D electron gas can be artificially realized. Compounds such as organic metals based on charge transfer salts are naturally low-dimensional electronic systems. They can usually be described in terms of a quasi-2D gas of electrons, i.e. they consist of highly conducting planes with a small electron hopping probability between the layers.

Features of the magnetic quantum oscillations of magnetization (de Haas-van Alphen effect) or of magnetoresistance (Shubnikov-de Haas effect) are known to be noticeably different in 2D systems compared to 3D systems. For example, the 2D de Haas-van Alphen effect is characterized by a sharp sawtooth-like shape at low temperatures, while the oscillations of the magnetization in 3D metals are always smooth [50].

In the 3D case each quantized Landau level can be represented in the reciprocal space as a cylindrical surface with generatrice parallel to the field direction and radius proportional to magnetic field. The de Haas-van Alphen effect consists in a periodic redistribution of electrons between strongly degenerated Landau levels when the radius of the cylinder corresponding to the upper filled Landau level crosses the Fermi surface radius. The cylindrical surfaces intersect the Fermi surface along some curve. All the points on this curve numerate the electronic states. The amount of these states (the length of the curve) changes gradually with magnetic field making the periodic process of redistribution of electrons between Landau levels more smooth. Hence these states act as a reservoir damping the influence of Landau quantization on magnetooscillatory phenomena. The discrete nature of the Landau levels is thus blurred due to the presence of these states inherent to the dimensionality of the spectrum. As a result, the chemical potential (the minimal energy needed to add an electron to the system) oscillations are strongly reduced in amplitude. Moreover, the oscillating part of the magnetoresistance is always small compared to the non-oscillating part.

In the 2D case, when all the electronic states of constant energy lay on lines in a plane, there are no additional states besides the discrete strongly degenerate Landau states, and thus the oscillations of the thermodynamic and transport properties can be very strong.

In quasi-2D systems, the situation concerning the energy spectrum is in some sense intermediate between the 2D and 3D cases and depends on the Landau level spacing $\hbar\omega_c = \hbar eH/m$ compared to the interlayer coupling energy t. At relatively small magnetic fields with $\hbar\omega_c < t$, the energy spectrum contains the dispersion of states along the magnetic field like for the 3D case leading to a broadening of the discrete density of states structure. At very high magnetic fields, the Landau levels are discrete with broadening only through the impurity scattering, exactly like in 2D systems. The (semiphenomenological) theory of the de Haas-van Alphen effect in quasi-2D systems reveals a crossover between the 2D and 3D limits for the behavior of the magnetization oscillations.

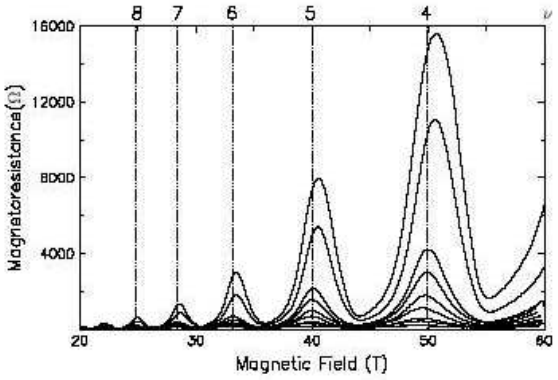

Figure 1.15: Oscillations of ρ_{zz} in the layered conductor $\beta''-(\mathrm{BEDT-TTF})_2\mathrm{SF}_5\mathrm{CH}_2\mathrm{CF}_2\mathrm{SO}_3$ at different temperatures (from the top, 0.59, 0.94, 1.48, 1.58, 1.91, 2.18, 2.68, 3.03, 3.38, 3.80, and 4.00 K). After Nam et al.

It is with the same idea of a reduction of the apparent dimensionality by the magnetic field that we have studied the magnetoresistance oscillations in quasi-2D systems [53]. We were rather interested in the limit of high magnetic fields, motivated by the experiment of Nam *et al.* [18] on the organic layered conductor $\beta''-(\mathrm{BEDT-TTF})_2\mathrm{SF}_5\mathrm{CH}_2\mathrm{CF}_2\mathrm{SO}_3$. Giant Shubnikov-de Haas oscillations of the longitudinal magnetoresistance ρ_{zz} have been observed at high magnetic fields and low temperatures (see the Fig. 1.15 taken from Nam et al.; here z is the direction of the magnetic field which is perpendicular to the layers). In particular, a regime with an exponential increase of the maxima of the magnetoresitivity ρ_{zz} for decreasing temperature has been pointed out for magnetic fields higher than 20 T. Such a feature is completely absent in the 3D Shubnikov-de Haas theory.

Another peculiar observation is that the saw tooth shape magnetization oscillations coexist with negligibly

[18] M.-S. Nam *et al.*, Phys. Rev. Lett. **87**, 117001 (2001)

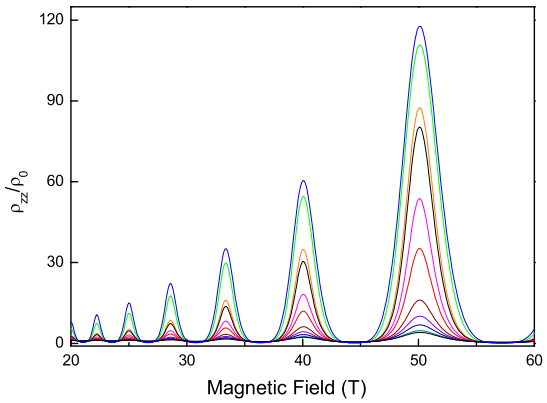

Figure 1.16: Calculated oscillations of ρ_{zz}/ρ_0 at different temperatures. ρ_0 is the residual resistivity at zero magnetic field and zero temperature.

small chemical potential oscillations in this material [19]. The reason for this is still unclear. An explanation may be the presence of an intrinsic non-quantized reservoir formed by quasi-1D bands of the Fermi surface. The reservoir of non-quantized states also helps to escape the problems related to the treatment of impurity scattering. The theory of quantum oscillation phenomena in this case was developed in [51].

Taking into account these points, our analytic calculations [53] developed in the framework of the quantum transport theory reveal a pseudo-gap structure in the spectral magnetoconductivity $\sigma_{zz}(\varepsilon)$ for energies between the Landau levels in high magnetic fields. In other words, when the energy of the electrons lies between the Landau levels, the conduction at a finite low temperature T is determined by the thermal excitation at the edges of the gap-like interval Δ between the levels. This explains why the minima of interlayer conductivity corresponding to the maxima of resistivity have a thermally activated dependence: $\sigma_{zz}^{\min} = (\rho_{zz}^{\max})^{-1} \sim \exp(-\Delta/T)$. At very low temperatures, quasi-particles whose energy lies in the pseudo-gap range Δ dominate the conduction, and the minima of conductivity saturate.

Our numerical calculations of ρ_{zz} at different finite temperatures shown in Fig. 1.16 reproduce well the appearance of huge oscillations in the same conditions of temperatures and magnetic fields as found experimentally. In particular we successfully obtain a thermal activation at the maxima of the longitudinal resistivity ρ_{zz} for fields $H \geq 20$ T.

[19] J. Wosnitza *et al.*, Phys. Rev. B **61**, 7383 (2000)